

Propagation of Surface Acoustic Pulses Generated by a Femtosecond Laser in Thin Films on Solid Substrates¹

Al. A. Kolomenskii,^{2,4} S. N. Jerebtsov,² and H. A. Schuessler²

The technique of phase velocity dispersion measurements of surface acoustic waves in a thin film-substrate system was demonstrated. The excitation of surface acoustic waves (SAWs) was quite efficient with femtosecond laser pulses, and the damage of the surface was minimized. The measurements were performed with films of Al deposited on silicon wafers. The errors in the determination of the phase velocity and absorption were analyzed. The temperature changes in the propagation velocity on bare Si wafers were also measured. The data obtained permitted estimation of the accuracy of the temperature determination from measurements with SAW pulses.

KEY WORDS: femtosecond laser generation; propagation velocity; silicon wafer; surface acoustic waves; temperature measurement.

1. INTRODUCTION

Surface acoustic waves (SAWs) represent a powerful tool for studies of elastic and mechanical properties of thin films [1]. These properties characterize the structure, homogeneity, and adhesion of a film to the substrate. The studies of films are important for different applications, such as microelectronics, protective coatings, and thin films for photovoltaics. With pulsed lasers the generated SAWs with frequencies up to several hundreds megahertz are readily available [2, 3]. These pulses can be detected with a

¹ Paper presented at the Fifteenth Symposium on Thermophysical Properties, June 22–27, 2003, Boulder, Colorado, U.S.A.

² Department of Physics, Texas A&M University, College Station, Texas 77843-4242, U.S.A.

³ General Physics Institute, Moscow 117942, Russia.

⁴ To whom correspondence should be addressed. E-mail: a-kolomenski@physics.tamu.edu

probe-beam-deflection method, piezoelectric foil detectors, or with an optical interferometer [1]. With surface acoustic gratings and diffraction detection, even SAWs of much higher frequencies can be studied [4]. The excitation can use the nondestructive thermoelastic mechanism or the destructive mechanism based on the laser ablation. With nanosecond laser pulses the second mechanism is usually more efficient. However, with femtosecond laser pulses efficient generation can be performed even in the thermoelastic excitation regime.

In the present paper we describe the principles of broadband SAW spectroscopy, perform the analysis of the signal-to-noise ratio for different modes of measurements, and present the results of measurements with films on solid substrates. Broadband excitation is carried out by a femtosecond laser.

2. THEORY

2.1. Propagation of SAWs in a Layered Structure of a Film on a Substrate

The problem of interest for analysis is the propagation of straight-crested SAWs in a system comprised of a film on a solid substrate. It is pertinent to SAW excitation with a laser focusing spot on the surface having the shape of a long strip. We assume that the media are non-piezoelectric and consider the acoustic field in the wave zone, where the excitation process is already completed, but the propagation distance is smaller than the diffraction length. In this case the divergence of the acoustic wave can be neglected. The particle displacements $u_k^{(n)}$ in each medium ($n = 1, 2$ correspond to the film and the substrate, respectively) are described by the set of equations of motion,

$$\rho^{(n)} \frac{\partial^2 u_j^{(n)}}{\partial t^2} - c_{ijkl}^{(n)} \frac{\partial^2 u_k^{(n)}}{\partial x_i \partial x_m} = 0, \quad (1)$$

where $\rho^{(n)}$ are the densities, $c_{ijkl}^{(n)}$ are the components of the elastic stiffness tensor, and the usual summation convention is assumed for the indexes i, j, k, l that accept values 1, 2, 3. The solutions of these equations can be sought as linear combinations of partial waves [5],

$$u_l^{(n)} = \alpha_l \exp(ikbx_3) \exp[ik(x_1 - ct)]. \quad (2)$$

Substitution of expressions of Eq. (2) into Eq. (1) gives a secular equation of sixth power for the determination of the possible values of b as functions of the SAW phase velocity c in each medium. There are three possible roots for b in the substrate that lie in the lower half of the complex

plane and assure the decay of the solutions with the depth. For the film all six roots are acceptable. Thus,

$$u_i^{(1)} = \sum_{\beta=1}^6 C_{\beta} \alpha_i^{(\beta)}(c) \exp[ikb_{\beta}(c) x_3] \exp[ik(x_1 - ct)], \quad (3)$$

$$u_i^{(2)} = \sum_{\beta=7}^9 C_{\beta} \alpha_i^{(\beta)}(c) \exp[ikb_{\beta}(c) x_3] \exp[ik(x_1 - ct)], \quad (4)$$

and the nine constants C_{β} should be chosen to satisfy the boundary conditions. The latter represent the following nine conditions: (1) at the surface of the film, which is assumed to be free, the components of stress must vanish; (2) the particle displacements and the components of stress at the two sides of the interface should be equal. Thus, the number of equations for determination of C_{β} corresponds to the number of equations following from the boundary conditions. This procedure can be generalized to the case of an arbitrary number of layers on the substrate, since each layer adds six constants, and at the same time, six additional boundary equations should be satisfied.

2.2. Determination of the Film Parameters

The measurement of a propagating and changing shape broadband SAW pulse at two distances permits determination of the frequency dependence of the attenuation α and the phase velocity c according to the formulas [6]:

$$\alpha = \frac{-\ln |A_2(x_2, f)/A_1(x_1, f)|}{x_2 - x_1} \quad \text{and} \quad c = \frac{2\pi(x_2 - x_1)}{\varphi_2(x_2, f) - \varphi_1(x_1, f)}, \quad (5)$$

where $A_{1,2}(x_{1,2}, f)$ and $\varphi_{1,2}(x_{1,2}, f)$ are the amplitudes and phases of the SAW pulse spectral components at distances $x_{1,2}$, respectively. The phase velocity depends on the dimensionless parameter $\gamma = kd$, where k is the wave number of the SAW spectral component and d is the thickness of the film. For $\gamma < 1$ the phase velocity can be expanded in a power series in γ :

$$c = c_0 + b_1\gamma + b_2\gamma^2 + \dots \quad (6)$$

When $\gamma \ll 1$ only a small portion of the SAW is contained in the film, and the dispersion of the phase velocity only slightly deviates from the linear dependence. Consequently, it can be described by two to three parameters that can be determined by fitting the theoretical model describing the propagation of SAWs in the system to experimental data. Then by

using the appropriate model, parameters of the substrate and optionally some additional data, such as the film thickness and material density of the film can be determined. With an increase of γ , the dependence becomes strongly nonlinear and additional parameters of the film can be evaluated from the measured data.

2.3. Estimates of the Signal-to-Noise Ratio

For detection with a probe beam deflection setup, the main contribution to the noise is produced by the shot noise [7]. The signal-to-noise ratio (SNR) can then be presented as

$$SNR = \left(\frac{2\pi^2 P \eta}{h\nu_L \Delta f} \right)^{1/2} M, \quad (7)$$

where P is the power of the laser beam at the surface, η is the quantum efficiency of the photodiode, ν_L is the frequency of light, Δf is the frequency range of the detection system, and $M = v_p/c$ is the acoustic Mach number equal to the ratio of the particle velocity v_p in the SAW to the propagation velocity c .

For the optimized SAW generation with the thermoelastic mechanism below the ablation threshold, estimates give SNR values of the order 1 to 10 for a single pulse. Then, by averaging over 10^4 pulses, one can obtain an estimate of $SNR \sim 10^2$ to 10^3 .

With an increase of the laser intensity and the onset of the ablation mechanism (as was observed in experiments with nanosecond pulses [8]), the amplitude of the SAW can be increased by a factor of 10^2 to 10^3 , so that $M \sim 10^{-4}$ to 10^{-3} can be obtained. Even higher amplitudes with M up to about 10^{-2} can be reached by using the excitation through a strongly absorbing layer [9]. Consequently, with these more efficient generation mechanisms the SNR can be improved even more; however, averaging is then limited by induced damage of the surface with repetitive laser action.

It should be noted that the phase measurements that are used for the determination of the phase velocity dispersion are not as sensitive to noise as are amplitude measurements. The signal can be presented as radius vectors with the amplitudes ($r_{1,2}$) and the phases ($\varphi_{1,2}$) at the two propagation distances $x_{1,2}$. The noise during the measurements is described by a random amplitude and phase (r_n, φ_n). We assume that $r_{1,2} \gg r_n$, which corresponds to $SNR = \min(r_{1,2}/r_n) \gg 1$ and is needed for accurate measurements. Then the relative error due to noise in the amplitude measurements is about $\delta_a = (SNR^{-1})$, while the error in the phase measurements is about $\delta_\varphi = (r_n/(2\pi r_{1,2}N))$, where N is proportional to the propagation

distance $N = (x_2 - x_1)/\lambda$. Here λ is the acoustic wavelength $\lambda = v/f$. Finally, we can present the errors in the phase velocity and attenuation measurements, respectively, as

$$\frac{\Delta c}{c} = \frac{1}{2\pi N SNR} \quad (8)$$

and

$$\Delta\alpha [Db/cm] = \left(\frac{20}{\ln(10)} \right) \frac{r_n}{(x_2 - x_1)} \frac{r_1 + r_2}{r_1 r_2}. \quad (9)$$

Since the propagation distance can be much larger than the acoustic wavelength (N is large), the error in phase measurements δ_n can be much smaller than the value of SNR^{-1} .

3. EXPERIMENTAL RESULTS

3.1. Setup

Our experimental setup used mode-locked Ti:sapphire laser seed generator pumped with a Spectra Physics Millennia diode-pumped solid state laser. The regenerative amplifier had two stages of amplification: a Spectra-Physics Spitfire pumped by the frequency doubled output of a Merlin laser and a TSA-25 pumped by the frequency doubled output of a Quanta-Ray Nd:YAG laser. The output of the Spitfire operated at 1 kHz had energy per pulse of about 1 mJ, and the output of the TSA-25 was at 10 Hz with the energy per pulse up to 30 mJ. In our measurements the energy used did not exceed 5 mJ. The duration of the laser pulses was about 60 fs, and the central wavelength was close to 800 nm. For the generation of SAWs with a plane front, the laser pulse was sharply focused with a cylindrical lens to a strip with a length ~ 10 mm and a width ~ 10 μ m. In phonon focusing measurements, the excitation beam was focused by a spherical lens to a spot with a diameter ~ 10 μ m.

The excited SAWs were registered with the probe-beam-deflection technique that could measure propagating pulses at two distances from the source in a single laser shot [9]. The upper limit for the power of the probe beam was set to avoid the melting of the sample surface and saturation of the photodiodes. The SAW pulse signal was registered in a wide frequency range with a digital oscilloscope (Tektronix TDS 680 C, 1 GHz real-time bandwidth).

3.2. Results

3.2.1. Excitation of Short SAW Pulses

With femtosecond laser pulses the excitation of powerful SAW pulses is possible even in the thermoelastic regime [10]. The development of the optical breakdown at the surface occurs after the deposition of the laser energy in the material has taken place. Consequently, the screening of the surface by the created plasma does not play a significant role, as it does with nanosecond laser pulses. For strongly absorbing materials it was observed that even with picosecond laser pulses the generation is more efficient than with nanosecond pulses at the same energy [11]. With the femtosecond generation less energy is required to produce SAW pulses with amplitudes significantly exceeding noise level. This results in smaller surface damage from ablation, and, therefore, it is possible to reproducibly generate many pulses at the same spot.

In Fig. 1 the pulse excited on (111)Si with the thermoelastic mechanism is shown. On a free surface of a metal, the ablation threshold is relatively low. The ablation can be prevented by covering the surface with a thin transparent liquid layer. For example, through a thin layer of a machine oil, a short and relatively high-amplitude pulse could be reproducibly and repetitively (many hundred times) excited in a polycrystalline stainless steel sample (Fig. 2).

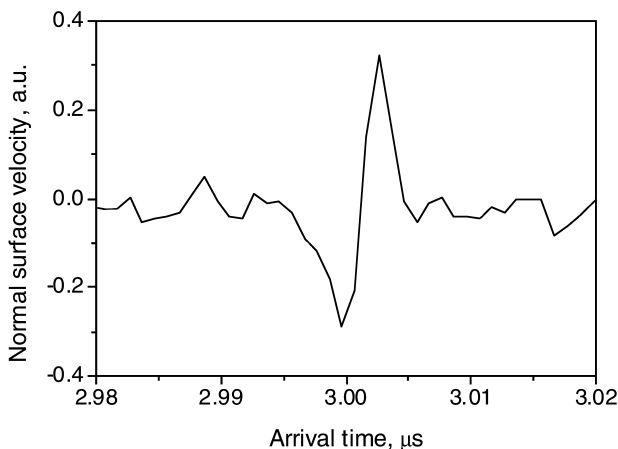


Fig. 1. SAW pulse excited at a free (100)Si surface and registered at the propagation distance $x = 15.4$ mm.

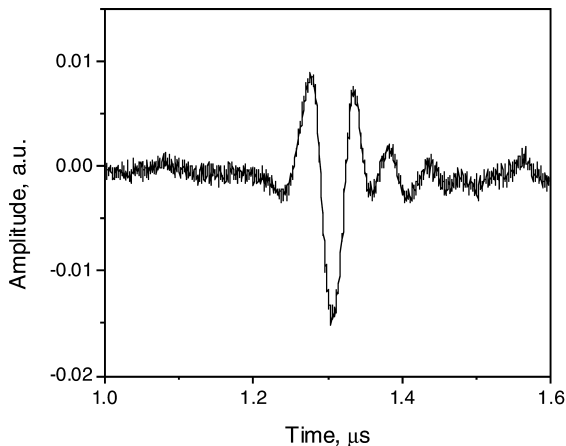


Fig. 2. Signal of a SAW pulse detected in stainless steel at $x = 3.8$ mm. The signal is averaged over 100 laser shots.

3.2.2. Propagation of SAW Pulses in Thin Films on Si Substrates

We studied the propagation of SAWs in samples consisting of a silicon substrate with a metallic film on it. Since silicon has a rather high propagation velocity of SAWs, the films that we studied corresponded to “loading” of the substrate and exhibited normal dispersion. Figure 3 shows a

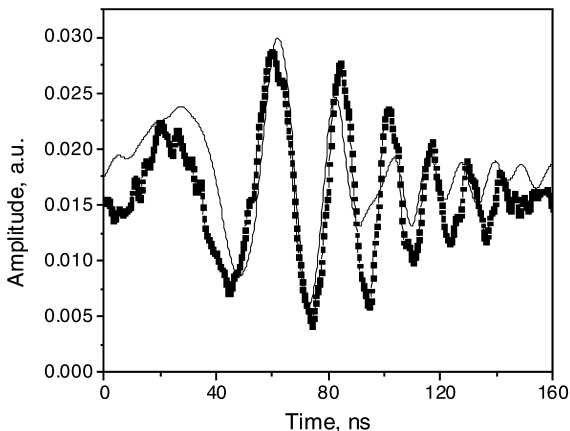


Fig. 3. Dispersive SAW pulse detected after propagating 17 mm. The system consists of (100)Si substrate with deposited aluminum film of $1 \mu\text{m}$ thickness. The solid line shows the result of the calculation with $c_0 = 5093 \text{ ms}^{-1}$, $b_1 = -0.11$, and $b_2 = -0.17$ (see Eq. (6)).

signal registered with aluminum film of 1 μm thickness at the second probe distance $x_2 = 17$ mm. We have also determined the dispersion coefficients for this film: $b_1 = -0.11 \pm 0.01$ and $b_2 = -0.17 \pm 0.02$ (see Eq. (6)) by fitting the shape of the pulse at the second distance when the shape of the pulse at the first probe spot ($x_1 = 4$ mm) was taken as the initial waveform in the calculation of the pulse evolution

3.2.3. Dependence of the Propagation Velocity on Temperature

A change of the temperature induces variations of the elastic properties and densities of both the film and the substrate. If, however, the initial difference in their parameters strongly exceeds temperature-created changes, the waveform of SAWs experiences a delay in the arrival time without drastic changes in the pulse shape. For relatively thin films ($kd \ll 1$ for all registered frequencies), most of the wave motion takes place in the substrate and, therefore, the changes in the elastic properties of the substrate contribute most to the overall variation of the propagation velocity. Figure 4 shows the velocity change with temperature for a bare silicon wafer with a (111) cut. Figure 5 shows temperature changes in the SAW propagation velocity for different angles on the (100) Si plane.

We have also measured the propagation velocity in the interval of angles where a phonon focusing effect was observed [12]. In this measurement the excitation laser beam was focused on the surface in a small spot by a spherical lens producing a point-like source on the (111)Si wafer. The amplitude dependence shows a small increase in the width of the

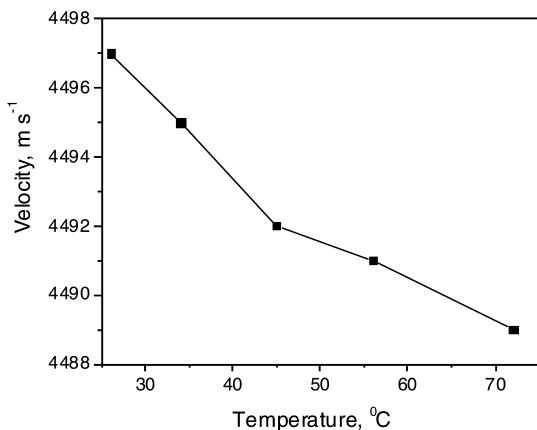


Fig. 4. Temperature dependence of the SAW propagation velocity on a bare (111)Si wafer in the direction $\langle 110 \rangle$.

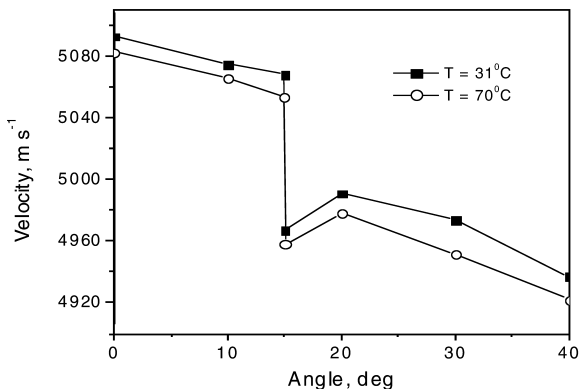


Fig. 5. Angular dependence of the SAW propagation velocity measured at two temperatures for (100)Si. The angle is measured from $\langle 010 \rangle$ direction.

amplitude maximum with increasing temperature (Fig. 6) corresponding to the change of the anisotropic angular dependence of the SAW phase velocity. This angular dependence is shown in Fig. 7 and was measured with the pump laser producing an extended line-like source. One can see that the main effect of the temperature increase on the phase velocity is a shift down of the velocity dependence as a whole with an increase of the temperature.

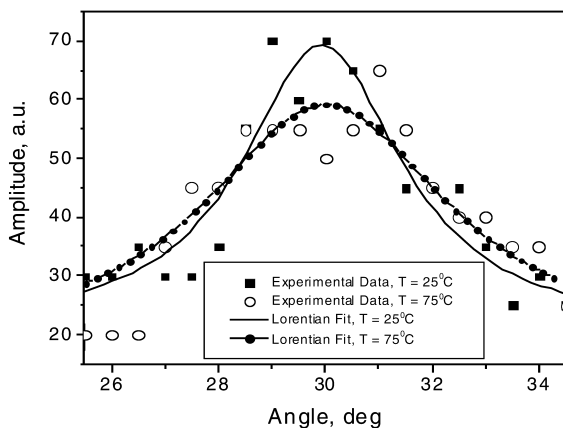


Fig. 6. Angular dependence of the SAW amplitude in the region of phonon focusing for two temperatures observed with a point-like source on a (111)Si wafer. The angle is measured from $\langle 110 \rangle$ direction.

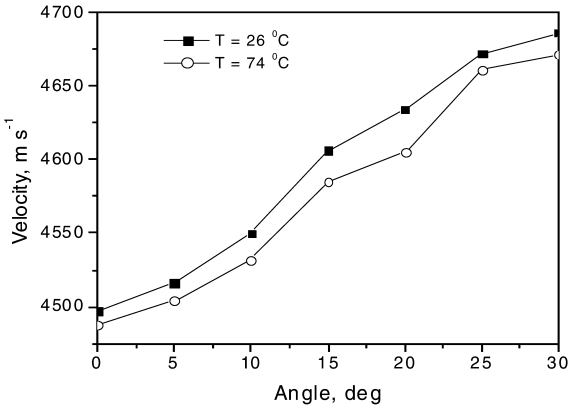


Fig. 7. Angular dependence of the SAW propagation velocity for two temperatures on a (111)Si wafer. The angle is measured from $\langle 110 \rangle$ direction.

From measured data we can estimate the accuracy of the temperature determination with SAW measurements. The error in the temperature determination is

$$\Delta T = c^2 \Delta t / [x |dc/dT|] \quad (10)$$

where x is the propagation distance and Δt is the temporal resolution of the pulse arrival time. In our measurements Δt was about 1 ns, and dc/dT is the slope of the phase velocity dependence on temperature. Estimating dc/dT from Fig. 4 for the (111) plane and from Fig. 5 for the (100) plane, we found for both planes $dc/dT \approx -0.2 \text{ m} \cdot \text{s}^{-1} \cdot \text{K}^{-1}$. Then the error of the temperature determination for silicon can be estimated as $\Delta t \sim 10 \text{ K}$.

4. CONCLUSIONS

We have implemented the pump-probe laser technique for SAW velocity measurements in a system of a thin film on a substrate. It was demonstrated that the excitation of SAWs is quite efficient with femtosecond laser pulses, and the damage of the surface can be minimized. The dispersive propagation of SAW pulses was observed with Al film deposited on a silicon wafer of (100) plane orientation. The errors in measurements of the SAW amplitude and phase relevant to determination of the absorption and phase velocity were analyzed. The temperature changes in the propagation velocity on bare Si wafers with (100) and (111) plane orientations were measured. With a sharply focused laser beam (point-like source) a

broadening with temperature increase of the amplitude peak in the vicinity of the phonon focusing direction on (111) plane was registered. The data obtained permitted estimation of the accuracy of the temperature determination from measurements with SAW pulses that for silicon was about 10 K.

ACKNOWLEDGMENTS

This material is based upon work supported by the National Science Foundation under Grants No. 9870143 and 9970241. We also thank A. A. Maznev for providing samples for this work and discussion of the results.

REFERENCES

1. P. Hess, *Physics Today* **55**:42 (2002).
2. A. A. Kolomenskii, M. Szabadi, and P. Hess, *Appl. Surface Sci.* **86**:591 (1995).
3. R. Kuschneireit, H. Fath, A. Kolomenskii, M. Szabadi, and P. Hess, *Appl. Phys. A* **61**:269 (1995).
4. R. M. Slayton, K. A. Nelson, and A. A. Maznev, *J. Appl. Phys.* **90**:4392 (2001).
5. G. W. Farnell and E. L. Adler, in *Physical Acoustics, Principles and Methods*, Vol. 9, W. P. Mason, ed. (Academic Press, New York, 1972), pp. 35–127.
6. A. Neubrand and P. Hess, *J. Appl. Phys.* **71**:227 (1992).
7. A. Van der Ziel, *Noise in Measurements* (Wiley, New York, 1976).
8. A. A. Kolomenskii and P. Hess, in *Proc. 1994 IEEE Int. Ultrasonics Symp.*, M. Levy, S. C. Schneider, and B. R. McAvoy, eds. (IEEE, New York, 1994), pp. 651–654.
9. Al. A. Kolomenskii and H. A. Schuessler, *Phys. Lett. A* **280**:157 (2001).
10. Al. A. Kolomenskii, S. N. Jerebtsov, and H. A. Schuessler, *Rev. Sci. Instrum.* **74**:453 (2003).
11. A. A. Kolomenskii and P. Hess, in *Proc. 15th Int. Cong. on Acoustics* (Trondheim, 1995), pp. 93–96.
12. Al. A. Kolomenskii and A. A. Maznev, *Phys. Rev. B* **48**:14502 (1993).